



**Environmental
Science**
Nano

Comparing the Fate of Pristine and Wastewater-Aged Gold Nanoparticles in Freshwater

Journal:	<i>Environmental Science: Nano</i>
Manuscript ID	EN-ART-02-2021-000156.R1
Article Type:	Paper

SCHOLARONE™
Manuscripts

ENVIRONMENTAL SIGNIFICANCE STATEMENT

An important process affecting the environmental fate of engineered nanomaterials (ENMs) is aggregation. Engineered surface coatings applied to ENMs during their manufacture have been shown to impact the aggregation of ENMs in synthetic and real waters. However, it is unlikely that ENMs released to the environment will resemble their ‘pristine’ form due to the myriad transformation processes that can alter an ENM’s physiochemical properties. Engineered systems, such as sewers and wastewater treatment plants, represent an important stage in the life-cycle of ENMs; it is expected that ENMs passing through these systems will be transformed prior to their incidental release to the environment. By directly comparing the aggregation behavior of ‘pristine’ and ‘wastewater-aged’ model ENMs with various engineered surface coatings, we find that the transformations of the ENMs occurring in wastewater media promote the homo- and heteroaggregation of the aged ENMs in freshwater media. This diverges from the aggregation behavior of the ‘pristine’ ENMs, which were generally resistant to homo- and heteroaggregation in freshwater. This work demonstrates the need to explicitly consider the transformations of ENMs when evaluating the factors and processes impacting their environmental fate.

1
2
3
4
5
6
7
8
9
10
11
12
13
14
15
16
17
18

Comparing the Fate of Pristine and Wastewater-Aged Gold Nanoparticles in Freshwater

19
20
21
22

Mark C. Surette^{1,2}, Campbell J. McColley¹, and Jeffrey A. Nason^{1*}*

23
24
25
26

¹ School of Chemical, Biological and Environmental Engineering
Oregon State University, 116 Johnson Hall, 105 SW 26th St., Corvallis, OR 97331

27
28
29
30
31
32

² Current Address: ORISE Postdoctoral Research Participant at U.S. EPA Center for
Environmental Measurement and Modeling
109 T.W. Alexander Drive, Research Triangle Park, NC 27709

33
34
35

* Corresponding Author: Jeff.Nason@oregonstate.edu

36
37
38
39
40
41
42
43
44
45
46
47
48
49
50
51
52
53

* Corresponding Author: Surette.Mark@epa.gov

ABSTRACT

The surface coatings applied to engineered nanomaterials (ENMs) during their manufacture have been shown to affect their aggregation behavior in aquatic media. This phenomenon has important implications on the environmental fate of ENMs and is often examined using ENMs in their 'pristine' form. However, the physiochemical properties of ENMs will be altered during their life cycle. Engineered systems, such as sewers and wastewater treatment plants, represent one pathway wherein ENMs can be transformed prior to their release. The focus of the current study was to compare the aggregation behavior of 'pristine' and 'wastewater-aged' ENMs in freshwater to provide insights into the impact of wastewater aging on ENM environmental fate. Gold nanoparticles (AuNPs) coated with polyethylene glycol (PEG), lipoic acid (COOH) and branched polyethylenimine (bPEI) were selected as model ENMs. The AuNPs were aged in filtered primary wastewater using a previously reported technique. The aged and pristine AuNPs were dosed into separate samples of raw and filtered freshwater and the loss of AuNPs from suspension by aggregation and sedimentation quantified using inductively coupled plasma mass spectrometry. Regardless of the initial surface coating, the AuNPs homoaggregated and acquired an organic matter corona while aging in the wastewater media. Following dispersion in the raw and filtered river water, the aged AuNPs were consistently lost from suspension. Greater loss was observed in the raw river water compared to the filtered river water, demonstrating that the aged AuNPs undergo heteroaggregation in addition to the homoaggregation that occurred during the aging process. This contrasts with the behavior of the pristine AuNPs, which were generally resistant to aggregation. These results indicate that while the physiochemical properties of the pristine AuNPs largely prevent their aggregation and subsequent sedimentation in the river water, the stabilizing effects of the engineered surface coatings examined in this study are lost after aging in wastewater. This demonstrates the importance of explicitly accounting for ENM transformations when designing experiments and selecting materials intended to elucidate the factors impacting ENM environmental fate.

INTRODUCTION

Engineered nanomaterials (ENMs) are being increasingly incorporated into a variety of consumer and industrial products.^{1, 2} While toxicological effects have been linked to some ENMs, the environmental risks they pose are not clear.^{3, 4} One challenge hindering ENM risk assessments is uncertainty regarding the concentration of ENMs in the environment. Due to analytical limitations, it is necessary to rely on environmental fate models to estimate exposure concentrations.⁵⁻⁷ However, the predicted environmental concentrations (PECs) generated by these models vary over several orders of magnitude.⁷ To reduce variability in these estimates, further refinement of ENM environmental fate models is necessary.

As noted by Garner et al. (2017)⁷, a key aspect of refining ENM environmental fate models is reducing the uncertainty of parameter values describing medium-dependent processes. One medium-dependent process that has received significant attention is the aggregation of ENMs in aquatic environments.⁸ This process can be affected by the surface coating applied to ENMs during their manufacture (herein referred to as “engineered surface coatings”) through a number of mechanisms, including electrostatic and/or steric forces.⁸⁻¹¹ The aggregation of ENMs can also be impacted by the adsorption of naturally-occurring organic macromolecules to the surface of the ENM, such as proteins, humic and fulvic substances.¹¹⁻¹³

The aggregation of ENMs is typically investigated using simulated aquatic media. While often yielding important mechanistic insights, there is growing recognition that the aggregation behavior of ENMs in simulated aquatic media, and the parameters describing this process, may diverge from their behavior in complex, natural aquatic media.^{8, 14-16} In these latter systems, the diverse array of organic macromolecules with varying chemical structure, bio- and geogenic colloids, and ionic species can alter ENM aggregation behavior in ways that are not reproduced in more simplistic aquatic media lacking these constituents.

Recent studies examining ENM aggregation behavior in complex aquatic media demonstrate the potential for engineered surface coatings to impact ENM environmental fate.¹⁶⁻¹⁸ Nonetheless, this process has generally been examined using ‘pristine’ ENMs.^{10, 19-21} It is widely recognized that

1
2
3
4
5 ENMs will be transformed during their life-cycle, resulting in materials that have significantly
6 different physiochemical properties than their pristine analogs.²² These transformation processes
7 can occur at various stages in an ENM's life-cycle and through a number of physical, chemical, and
8 biological processes.²²⁻²⁵ This raises the question of whether the aggregation behavior of 'aged'
9 ENMs differs from the behavior of their more often studied pristine analogs, particularly within
10 real aquatic media.
11
12
13
14
15

16
17 When considering the life-cycle of ENMs, engineered systems such as sewers and wastewater
18 treatment plants (WWTPs) represent an important stage where an ENM's physiochemical
19 properties can be altered.²⁶⁻³⁴ While research has shown that the majority of ENMs entering these
20 engineered systems will be removed, their complete removal is unlikely and, therefore, WWTP
21 effluent represents one pathway through which ENMs will be released to the environment.³⁰⁻³⁵ Thus,
22 it is critical to understand the properties and aggregation behavior of ENMs following their
23 passage through such systems. At present, it is unclear whether the properties of engineered
24 surface coatings remain a relevant factor influencing ENM environmental fate after the ENMs
25 have been transformed in wastewater treatment systems.
26
27
28
29
30
31
32

33
34 The focus of the current work was to examine the impact of wastewater aging on ENM
35 aggregation behavior in freshwater media. Three different types of 15 nm gold nanoparticles
36 (AuNPs), each with a different covalently bound (thiol) engineered surface coating, were used as
37 model ENMs. These engineered surface coatings were previously found to alter ENM aggregation
38 in real and simulated freshwater media, as well as the ENM transformations during conventional
39 wastewater treatment processes.^{17, 36, 37} These AuNP types were also shown to undergo rapid
40 transformations in wastewater, with an organic matter corona acquired during exposure to the
41 influent wastewater that persisted even as the aquatic chemistry of the matrix changed.³⁷ Based
42 on these findings, filtered effluent from the primary clarifier of a full-scale WWTP was used to age
43 the AuNPs in this work. Using 'pristine' and 'aged' variants of each AuNP type, a suite of batch
44 experiments was performed to compare changes in the suspended AuNP concentration over time.
45 Samples of raw and filtered river water were used to explore the effect of homoaggregation alone
46 (filtered) and the combined effects of homo- and heteroaggregation (raw). A suite of
47
48
49
50
51
52
53
54
55

1
2
3
4
5 complementary techniques was used to characterize the pristine and aged AuNPs and to further
6 examine their aggregation behavior in the various media used.
7
8
9

10 In building on the previous investigations, the results from the current research help to establish
11 the capacity for engineered surface coatings to alter ENM environmental fate under highly
12 realistic conditions. Ultimately, this work aims to help identify the dominant factors influencing
13 ENM aggregation behavior in order to accelerate the refinement of ENM environmental fate
14 models.
15
16
17
18
19

20 **MATERIALS AND METHODS**

21 **Engineered Nanomaterials**

22 Three different types of 15 nm gold nanoparticles (AuNPs), each with a different covalently bound
23 (thiol) engineered surface coating, were used as model ENMs: 5 kiloDalton (kDa) polyethylene
24 glycol (PEG), lipoic acid (COOH), and 25 kDa branched polyethylenimine (bPEI). All the AuNPs were
25 purchased from nanoComposix, Inc. (NanoXact 0.05 mg/mL). The measured and manufacturer
26 reported characteristics of the pristine AuNPs are provided in Table 1. Further details regarding
27 their characterization, including the conversion of the measured electrophoretic mobility (μ_E) to
28 the modelled zeta potential (ζ) values, are provided in the Supplementary Information.
29
30
31
32
33
34
35
36
37
38
39
40
41
42
43
44
45
46
47
48
49
50
51
52
53
54
55
56
57
58
59
60

Table 1. Measured and manufacturer reported properties of pristine AuNPs.

Surface Coating	Core Diameter (D_c) [nm]	Intensity-Weighted Hydrodynamic Diameter ($D_{h,o}$) [nm]	Electrophoretic Mobility (μ_E) [$\mu\text{m/s}$ / (V/cm)]	Zeta Potential (ζ) [mV]	Surface Plasmon Resonance (λ_{SPR}) [nm]
PEG	15.4 \pm 1.1	40.0 \pm 1.76	-0.28 \pm 0.17	-5.9 \pm 3.6	519.2 \pm 1.9
COOH	15.4 \pm 1.2	16.8 \pm 4.9	-0.98 \pm 0.2	-20.6 \pm 4.2	518.5 \pm 5.4
bPEI	15.3 \pm 1.1	26.1 \pm 3.6	0.56 \pm 0.13	11.8 \pm 2.7	521.5 \pm 2.2

Error bars indicate \pm 95% confidence interval (D_c : $n = N/R$; $D_{h,o}$: $n = 3$; μ_E/ζ : $n = 15$; λ_{SPR} : $n = 3$).

Electrophoretic mobility measured at pH \approx 7.4 in pH-adjusted 1 mM KCl; others measured in DDI water.

D_c : Manufacturer reported; $D_{h,o}$, μ_E , and λ : measured. See Supplementary Information for details.

River Water

Samples were collected from the Willamette River (Oregon, USA) as described previously.¹⁷ Briefly, approximately 2 L samples of river water were collected from the intake line to the City of Corvallis' municipal drinking water treatment facility (H.D. Taylor Water Treatment Plant, Corvallis, OR) using acid-washed 1 L high-density polyethylene (HDPE) containers (Nalgene). The samples were collected between 8:30 – 9:30 a.m. on the day of the batch experiments (detailed below). Shortly after collection, half of the sample was sequentially filtered through pre-rinsed 0.45 μm and 0.2 μm Supor membrane filters (Pall Corporation) and stored in the dark at 4 $^\circ\text{C}$ until use (referred to herein as filtered river water). Each filter was pre-washed with >125 mL of 18.2 M Ω -cm distilled, deionized (DDI) water (EGLA Purelab) prior to use and the initial (>25 mL) filtrate was discarded. The remainder of the river water was unaltered (referred to herein as raw river water). Additional details on the collection, preparation, and analysis of the river water can be found in the Supporting Information. A summary of the water quality characteristics of the river water used in each group of batch experiments is provided in Table 2 (see Supplementary Information Table S2 for details).

Table 2. Water quality characteristics of Willamette River water used in batch tests.

Parameter	Value			Units
	Feb. 25 th (PEG)	March 5 th (bPEI)	March 15 th (COOH)	
Dissolved Organic Carbon (DOC)	2.47 ± 0.04	1.63 ± 0.04	1.49 ± 0.06	mg C/L
Ionic Strength	0.81	0.96	0.92	mM
pH	7.39	7.32	7.22	
Total Suspended Solids (TSS)	104.6 ± 5.2	13.7 ± 11.2	11.3 ± 6.3	mg/L
Total Alkalinity	20.31	23.20	23.95	mg/L as CaCO ₃
Total Hardness	18.06 ± 0.87	22.26 ± 0.54	21.3 ± 2.22	mg/L as CaCO ₃

Error bars indicate ± 95% confidence interval ($n = 3$).

Dialyzed and Synthetic River Water

As both natural organic matter (NOM) and ionic species in river water can influence the aggregation behavior of ENMs, two types of synthetic aquatic media were prepared to separately investigate each of these factors. To examine the impacts of NOM, an aliquot of the filtered river water was dialyzed over a 7-day period to remove salts and isolate the NOM in the Willamette River water. A 150 mL aliquot of the filtered river water was sealed in 3.5 kDa molecular weight cut-off (MWCO) regenerated cellulose dialysis tubing (Fisherbrand) and submerged in DDI water. Twice a day, the conductivity of the surrounding DDI water was measured and then replaced with fresh DDI. The dialysis process was considered complete when the conductivity of the surrounding DDI water was consistent, eventually measuring $1.26 \pm 0.25 \mu\text{S}/\text{cm}$ ($\pm 95\%$ confidence interval; $n = 5$) in the final five measurements. The DOC of the dialyzed river water was measured per the method detailed in the Supplementary Information and was found to be $1.86 \pm 0.06 \text{ mg C/L}$ ($\pm 95\%$ confidence interval; $n = 3$), which is comparable to the average DOC of the river water samples used in the batch experiments (Table 2). To investigate the impact of ionic species, a synthetic river water was prepared to match the average concentration of the major ionic species measured in the samples of Willamette River water used in the batch experiments (Supplementary Information Table S2). The composition of the major ionic species was obtained by combining the requisite amount of NaHCO_3 , CaCl_2 , CaCO_3 , MgCl_2 , MgSO_4 , and KNO_3 in DDI water to produce the average concentration of HCO_3^- , Ca^{2+} , and Mg^{2+} measured in the Willamette

1
2
3
4
5 River water (Supplementary Information Table S2) while maintaining comparable ionic strength
6 (Table 2). The ionic strength of the synthetic river water (1.07 mM) was estimated based on the
7 measured conductivity and compared to that measured for the Willamette River water (Table 2).
8
9 Details on the actual ionic composition of the synthetic river water are provide in the
10 Supplementary Information (Table S3). The dialyzed and synthetic river water were stored in the
11 dark at 4 °C until use.
12
13
14
15
16

17 **Engineered Nanomaterial Aging**

18 The model ENMs were aged in effluent from the primary clarifier of a full-scale municipal
19 wastewater treatment facility based on a procedure outlined previously.³⁷ Briefly, approximately
20 2 L samples of primary clarifier effluent were collected using acid-washed 1 L high-density
21 polyethylene (HDPE) containers (Nalgene). The samples were collected between 8:45 – 9:30 a.m.
22 on the day of the batch experiments (detailed below). To remove the suspended solids, the
23 wastewater samples were first centrifuged at $\approx 1,800g$ RCF for 30 minutes. The supernatant (≈ 1.8
24 L) was then decanted and sequentially filtered through pre-rinsed and ashed 1.2 μm glass
25 microfiber filter (GF/C Whatman) followed by pre-rinsed 0.45 μm and 0.2 μm Supor membrane
26 filters (Pall Corporation). Each filter was pre-washed with >125 mL of DDI water prior to use and
27 the initial (>25 mL) filtrate was discarded. The filtered wastewater samples were stored in the
28 dark at 4 °C until use. A summary of the water quality characteristics of the wastewater samples
29 used in each group of batch experiments is provided in Table 3 (see Supplementary Information
30 Table S4 for details).
31
32
33
34
35
36
37
38
39
40
41

42 To generate the aged ENMs, 245 mL of filtered wastewater was dosed with 5 mL of a given pristine
43 AuNP type to an initial concentration of 1 mg Au/L. The AuNPs were allowed to incubate in the
44 wastewater matrix for ≈ 30 minutes before the AuNP/wastewater dispersion was concentrated
45 using a VivaFlow 50R 100 kDa MWCO tangential-flow filtration (TFF) cartridge (Sartorius). Based
46 on initial testing, the 100 kDa MWCO membrane was found to maintain the AuNPs within the
47 retentate while allowing the excess wastewater matrix to pass through the membrane (see
48 Supplementary Information for details; Table S5). During the concentration/separation process,
49 the AuNP/wastewater dispersion was continuously circulated through the TFF cartridge at a
50
51
52
53
54
55
56
57
58
59
60

flowrate of 100 mL/minute and a transmembrane pressure (TMP) of ≈ 2 bar. This process was continued until the permeate volume, which was tracked gravimetrically, was $\geq \approx 225$ mL (corresponding to a concentration factor of $\geq 10^1$). A portion of the concentrated aged AuNP dispersion was immediately used in the batch experiments (detailed below). The remainder was stored at 4 °C in the dark and used the following day (<12 hours later). During this storage period, the size of the aged AuNPs did not substantially change (Table S6). Additional details regarding the testing and storage of the TFF cartridge are provided in the Supplementary Information.

Table 3. Water quality characteristics of primary clarifier effluent used in batch tests.

Parameter	Value			Units
	Feb. 26 th (PEG)	March 6 th (bPEI)	March 16 th (COOH)	
Dissolved Organic Carbon (DOC)	10.2 \pm 0.87	16.42 \pm 0.61	17.66 \pm 0.48	mg C/L
Ionic Strength ^a	8.4	9.2	9.1	mM
pH	6.87	7.08	7.61	
Conductivity	523.0	574.0	570.0	μ S/cm

^a Estimated per $l = 1.6 \times 10^{-5}$ Specific Conductance (S.C.)³⁸
Error bars indicate \pm 95% confidence interval ($n = 3$).

Batch Experiments

Batch experiments were performed to assess the aggregation behavior of each AuNP type/form in the raw and filtered river water. The overall approach used during the batch experiments is similar to that reported previously¹⁷ and the reader is referred therein for additional details supporting the experimental design. An illustration depicting the experimental approach is shown in the Supplementary Information Figure S1. For each AuNP type, four different groups of batch experiments were performed: pristine AuNPs in raw river water, pristine AuNPs in filtered river water, aged AuNPs in raw river water, and aged AuNPs in filtered river water. Each group included six replicates of the selected AuNP type/matrix combination, as well as two controls—raw river water centrifuged at 3,500 rpm ($\approx 2,200g$ RCF) for 5 minutes (referred to herein as centrifuged river water) and DDI water. The filtered river water was used to examine the impact of homoaggregation in isolation while the raw river water was used to assess the combined impact

1
2
3
4
5 when both homo- and heteroaggregation can occur. The centrifuged river water was also used to
6 assess the combined impact of both homo- and heteroaggregation but was focused on examining
7 the effect of small naturally occurring colloids (NCs; $d_{NC} < \approx 300$ nm) on the AuNP
8 heteroaggregation behavior. As was demonstrated previously, the centrifugation speed and
9 duration used to prepare the centrifuged river water removes relatively large background NCs
10 while leaving small NCs in suspension.¹⁷ For this reason, the centrifuged river water represents an
11 intermediate NC concentration between the raw and filtered river water, with the number
12 concentration of background NCs highest in the raw river water and lowest in the filtered river
13 water. The DDI water control was used to assess vessel interactions and the loss of the AuNPs
14 during the centrifugation step.
15
16
17
18
19
20
21
22

23 Using 50-mL polypropylene centrifuge tubes (VWR International), each group of eight vials (i.e.,
24 six replicates and two controls) were prepared by dosing the selected matrix to a target initial
25 concentration ($C_{NP,initial}$) of 250 $\mu\text{g Au/L}$. After dosing, each vessel was briefly vortexed and a 5 mL
26 aliquot was collected to measure $C_{NP,initial}$. The vials were then placed horizontally on a shaker table
27 and continuously mixed at 200 rpm for 60 minutes. After mixing, the vessels were immediately
28 centrifuged at 3,500 rpm ($\approx 2,200g$ RCF) for 5 minutes and the supernatant ($V_{TOT} = 30$ mL) was
29 collected to measure the concentration of AuNPs remaining in suspension ($C_{NP,final}$) via three
30 sequential withdrawals of 10-mL aliquots collected ≈ 1 cm below the surface. Each sample was
31 digested using *aqua regia* (3:1 ultrapure HCl:HNO₃) and the AuNP concentration was measured
32 using an Agilent 7900 inductively-coupled plasma mass spectrometer (ICP-MS; Agilent
33 Technologies). Additional details regarding the digestion technique are provided in the
34 Supplementary Information.
35
36
37
38
39
40
41
42
43
44

45 **Supporting Analytics**

46 Time-resolved dynamic light scattering (TR-DLS) was used to assess the colloidal stability of the
47 pristine AuNPs in filtered river water. The intensity-weighted hydrodynamic diameter (D_h) of the
48 AuNPs was measured for ≈ 30 minutes at $C_{NP} = 1$ mg Au/L and the extent of aggregation ($D_{h,30}/D_{h,0}$)
49 was calculated. Values of $D_{h,30}/D_{h,0} \approx 1.0$ denote particle stability whereas $D_{h,30}/D_{h,0} > 1.0$ indicates
50 aggregation. Phase analysis light scattering (PALS) was used to measure the electrophoretic
51
52
53
54
55
56
57
58
59
60

1
2
3
4
5 mobility (μ_E) of the pristine AuNPs in filtered river water at $C_{NP} = 5$ mg Au/L. Conformational
6 changes to the pristine engineered surface coating and/or the adsorption of organic
7 macromolecules to the surface coating were examined in filtered river water at $C_{NP} = 5$ mg Au/L
8 using ultraviolet-visible light spectroscopy (UV-Vis). The pristine AuNP concentrations used during
9 the PALS and UV-Vis measurements were chosen to generate adequate signals using these
10 techniques.
11
12
13
14
15

16
17 The aged AuNPs were also characterized via DLS, PALS, and UV-Vis in filtered river water and the
18 wastewater permeate generated during each aging procedure (TFF permeate). Due to the lower
19 concentration of the aged AuNP/wastewater dispersion (≈ 5 mg Au/L; see Supplementary
20 Information Table S5), the DLS, PALS, and UV-Vis measurements of the aged AuNPs were
21 performed at ≈ 1 mg Au/L. The colloidal stability of the aged AuNPs was also examined via TR-DLS
22 in the filtered river water, dialyzed river water, and synthetic river water to systematically
23 investigate the mechanisms driving the aggregation behavior of the aged AuNPs. The D_h of the
24 aged AuNPs was measured for ≈ 60 minutes at $C_{NP} \approx 1$ mg Au/L and the extent of aggregation
25 ($D_{h,60}/D_{h,0}$) was calculated. The duration of the TR-DLS measurements was increased (relative to
26 those performed using pristine AuNPs) to match the duration of the batch experiments. Further
27 details regarding the preparation and analysis of the samples via these methods have been
28 discussed previously and are summarized in the Supplementary Information.^{17, 37}
29
30
31
32
33
34
35
36
37

38
39 Lastly, samples of the pristine and aged AuNPs in the raw, centrifuged, and filtered river water
40 were analyzed via scanning electron microscopy (SEM) using a Zeiss Sigma VP scanning electron
41 microscope (Zeiss Microscopy). The microscope was operated at an acceleration voltage of 5 kV
42 and micrographs were obtained using the InLens detector. Samples of each AuNP type/form in
43 each variant of river water (i.e., raw, centrifuged, and filtered) were prepared by collecting a 1.5
44 mL aliquot from one of the batch experiments after mixing but prior to centrifugation. The aliquot
45 was transferred to a polystyrene micro-centrifuge tube (VWR) containing an unfunctionalized
46 carbon grid (Cu 200 mesh, carbon coated; Ted Pella) mounted on an aluminum support cone. The
47 sample was then centrifuged at 14,000 rpm ($\approx 26,000g$ RCF) for 30 minutes, after which the grid
48 was removed and dried overnight under vacuum.
49
50
51
52
53
54

RESULTS AND DISCUSSION

For each AuNP type/matrix combination, Figure 1 presents the concentration of AuNPs remaining in suspension at the completion of the batch experiment ($C_{NP,final}$) compared to the initial AuNP concentration ($C_{NP,initial}$). Statistical differences were determined using a one-way paired t -test ($\alpha = 0.05$; n varies). A decrease in the AuNP concentration was attributed to the aggregation and subsequent settling of the AuNPs (herein termed loss and denoted as η), while no change in the AuNP concentration indicated that the AuNPs were stable and resistant to aggregation and settling. In the batch tests using the filtered river water, the loss of the AuNPs was attributed to their homoaggregation and subsequent settling, whereas loss in the raw river water was attributed to a combination of homo- and heteroaggregation due to the presence of natural colloids. Greater loss of the AuNPs in the raw river water when compared to the filtered river water was attributed to heteroaggregation.

Pristine AuNPs in River Water

PEG-AuNPs: The loss of the pristine PEG-AuNPs was significant in the raw river water (paired *t*-test [$n = 5$], $p < 0.01$; Figure 1a) but was not significant in the filtered river water (paired *t*-test [$n = 6$], $p = 0.49$; Figure 1c). The pristine PEG-AuNPs were also lost from suspension in the centrifuged river water (Figure 1b), albeit to a lesser extent than the raw river water ($\eta \approx 29\%$ vs. 35% , respectively), and negligible losses were observed in DDI water (Figure 1d; $\eta \approx 6\%$). In combination, these results indicate that the pristine PEG-AuNPs heteroaggregated with the NCs in the raw and centrifuged river water while being resistant to homoaggregation. This is further supported by the negligible loss observed in DDI water, indicating that adsorption to the vessel walls or removal via the centrifugation process was minimal.

The behavior of the pristine PEG-AuNPs in the raw river water contrasts with our previous results.¹⁷ However, given that the total suspended solids (TSS) concentration of the raw river water used in the PEG-AuNP batch experiments (Table 2) was considerably higher than the previous study (104.6 ± 5.2 mg/L vs. 3.9 ± 0.4 mg/L, respectively), the increased loss is reasonable given the second-order dependence of aggregation on particle number concentration. Due to the lower background NC concentration, as well as differences in the experimental approach, it is possible that heteroaggregation of the pristine PEG-AuNPs in the previous study went undetected. It is also possible that the size distribution and chemical characteristics of the NCs were different in the previous study, as the river water sample for the current work was collected after a rain event, which may have affected interactions between the pristine PEG-AuNPs and background NCs. In any case, the TR-DLS, PALS, and UV-Vis measurements of the pristine PEG-AuNPs in the filtered river water were consistent with our previous findings^{17,36}, confirming that steric interactions between the PEG-AuNPs prevented their homoaggregation in the river water (Figure 2a and Supplementary Information Figure S2a) while the negative surface charge of the PEG surface coating prevented the adsorption of NOM (Figure 2b and Supplementary Information Figure S4 and Tables S8 – S9). The SEM micrographs confirm the trends

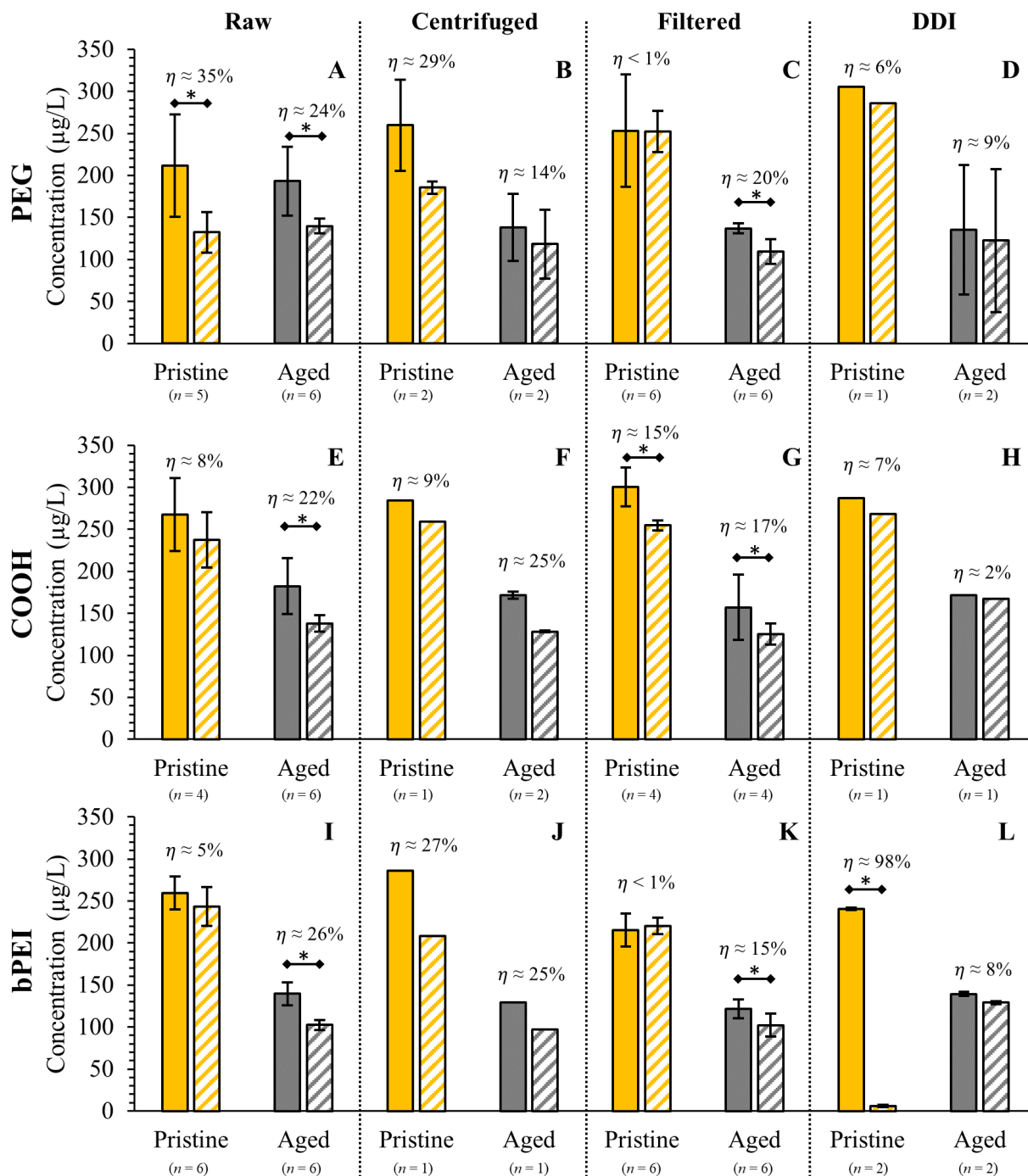


Figure 1. $C_{NP,initial}$ (solid) and $C_{NP,final}$ (hashed) for each AuNP type/form in raw river water, centrifuged river water, filtered river water, and DDI water. Error bars indicate ± 1 S.D. (n varies, as indicated). Asterisks indicate significant decreases in concentration (one-way paired t -test; $\alpha = 0.05$; limited to the raw and filtered river water due to sample size).

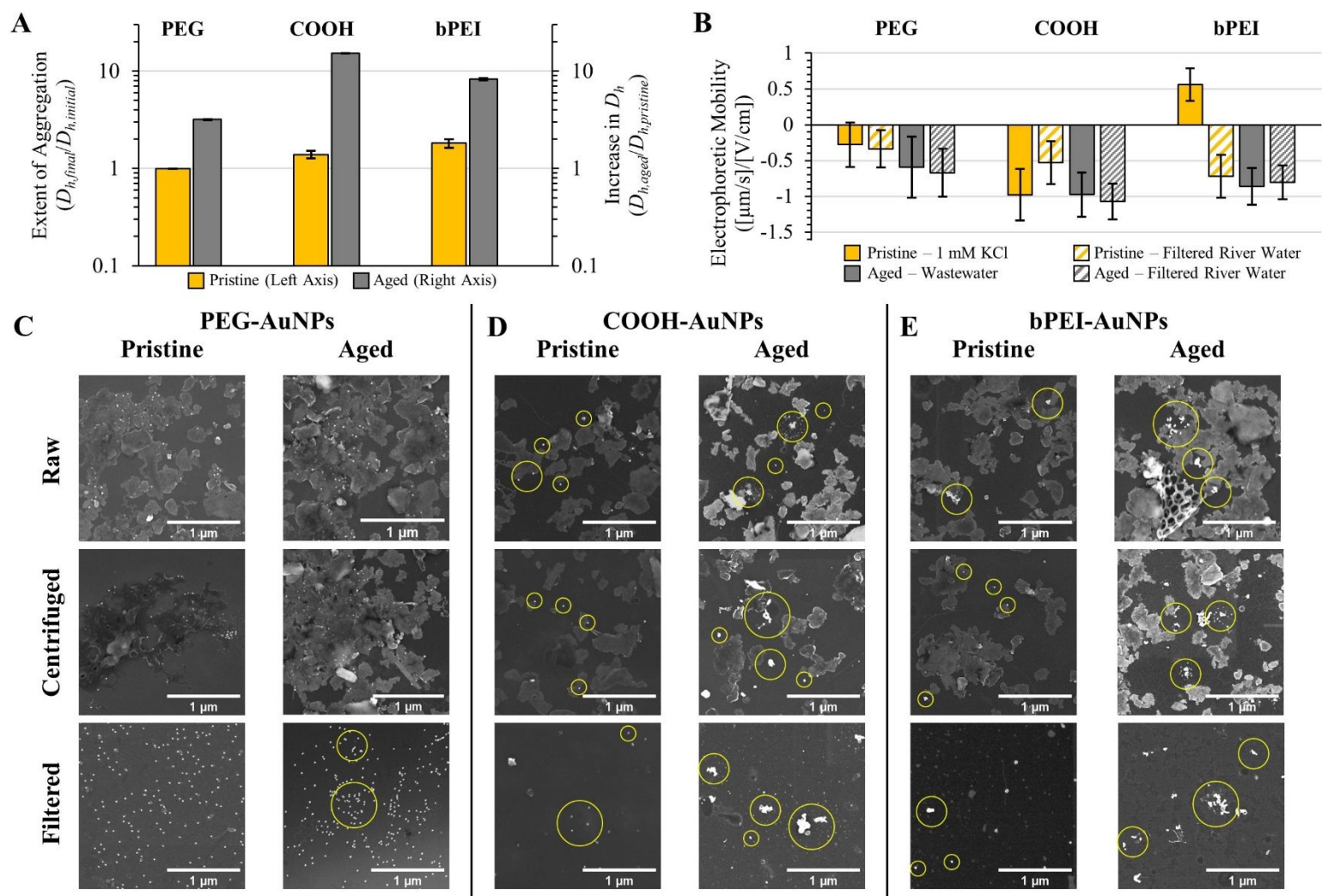


Figure 2. (A) Extent of aggregation ($D_{h,final}/D_{h,initial}$) of pristine AuNPs in filtered river water (gold) and increase in D_h of aged AuNPs relative to D_h of pristine AuNPs ($D_{h,aged}/D_{h,pristine}$) measured in DDI water (grey); (B) electrophoretic mobility (μ_E) of pristine AuNPs in pH-adjusted 1 mM KCl (solid gold; pH \approx 7.4), pristine AuNPs in filtered river water (hashed gold; pH 7.2 – 7.4, see Table 2), aged AuNPs in wastewater permeate (solid grey; pH 6.9 – 7.6, see Table 3), and aged AuNPs in filtered river water (hashed grey; pH 7.2 – 7.4, see Table 2); and (C-E) SEM micrographs of each AuNP type/form in raw

1
2
3 (top), centrifuged (middle) and filtered (bottom) river water (circular call-outs indicate AuNPs; larger micrographs presented in Supplementary
4 Information Figures S5 – S10). Error bars indicate ± 1 S.D. with **(A)** pristine: $n = 2$, aged: $n = 3$ and **(B)** $n = 15$.
5
6
7
8
9
10
11
12
13
14
15
16
17
18
19
20
21
22
23
24
25
26
27
28
29
30
31
32
33
34
35
36
37
38
39
40
41
42
43
44
45
46
47

1
2
3
4
5 observed in both the batch experiments and the supplementary analytical techniques, indicating
6 that the pristine PEG-AuNPs heteroaggregated with the background NCs in the raw and
7 centrifuged river water while remaining dispersed and unaggregated in the filtered river water
8 (Figure 2c).
9
10
11

12
13
14 *COOH-AuNPs*: The loss of pristine COOH-AuNPs from suspension was not significant in the raw
15 river water (paired t -test [$n = 4$], $p = 0.22$; Figure 1e) but was significant in the filtered river water
16 (paired t -test [$n = 4$], $p = 0.02$; Figure 1g). The loss of the pristine COOH-AuNPs in the filtered river
17 water ($\eta \approx 15\%$) was slightly greater than that measured in the raw and centrifuged river water,
18 as well as the DDI water, all of which were comparable ($\eta \approx 8\%$, 9% and 7% ; Figure 1e, 1f, and 1h,
19 respectively). These results suggest that the pristine COOH-AuNPs were susceptible to
20 homoaggregation, yet resistant to heteroaggregation with the background NCs. As with the PEG-
21 AuNPs, the negligible loss observed in DDI water indicates that adsorption to the vessel walls or
22 removal via the centrifugation process was minimal.
23
24
25
26
27
28
29

30
31 The behavior of the pristine COOH-AuNPs in both the raw and filtered river water was consistent
32 to that observed in the previous study.¹⁷ Nonetheless, the exact mechanism causing the pristine
33 COOH-AuNPs to homoaggregate remains unclear. The TR-DLS measurements in the filtered river
34 water indicate a small initial increase in D_h , after which no further changes occurred (Figure 2a
35 and Supplementary Information Figure S2b). While suggestive of a small degree of
36 homoaggregation, previous work in simulated and filtered river water demonstrated that
37 electrosteric interactions between the COOH-AuNPs prevent this.^{17, 36} The increase in D_h could
38 also be due to the rapid adsorption of NOM. However, the UV-Vis measurements provide
39 conflicting information, as no significant change in the λ_{SPR} was measured in the filtered river
40 water relative to that measured in DDI water (Supplementary Information Figure S4b and Table
41 S8) but do show an increase in the full-width at half-max (FWHM; Supplementary Information
42 Table S9), suggesting that the particles were transformed. Due to the negative surface charge of
43 the COOH-AuNPs (Supplementary Information Figure S4), electrostatic interactions with NOM
44
45
46
47
48
49
50
51
52

1
2
3
4
5 macromolecules would be unfavorable. The SEM micrographs in the raw, centrifuged, and filtered
6 river water indicate that the pristine COOH-AuNPs were unaggregated, as individual
7 monodispersed AuNPs are evident in each of the media variants (Figure 2d). While some of the
8 COOH-AuNPs in the raw and centrifuged river water appear to be attached to the background
9 NCs, others are monodispersed and separate from the NCs. Thus, the close proximity of some of
10 the COOH-AuNPs to the background NCs is likely an artifact of the sample preparation rather than
11 indicative of heteroaggregation (unlike the PEG-AuNPs in the raw and centrifuged river water,
12 which were only found on the background NCs [Figure 2c]). In summary, the results provide
13 consistent evidence that the pristine COOH-AuNPs were resistant to heteroaggregation while
14 contradictions in the data do not provide clear evidence of the mechanism driving the loss of the
15 pristine COOH-AuNPs in the filtered river water.
16
17
18
19
20
21
22
23
24

25 *bPEI-AuNPs*: The loss of the pristine bPEI-AuNPs was not significant in either the raw river water
26 (paired t -test [$n = 6$], $p = 0.17$; Figure 1i) or filtered river water (paired t -test [$n = 6$], $p = 0.3$; Figure
27 1k). While a decrease in the concentration of the pristine bPEI-AuNPs was measured in the
28 centrifuged river water (Figure 1j), this was based on a single measurement. Unlike the other
29 three aquatic media, significant losses were observed in the DDI water ($\eta \approx 98\%$; Figure 1l),
30 indicating the pristine bPEI-AuNPs adsorbed to the vessel walls, likely due to the absence of the
31 NOM in the river water (discussed further below). In combination, these results suggest that the
32 pristine bPEI-AuNPs were resistant to both homo- and heteroaggregation in the river water.
33
34
35
36
37
38
39

40 The behavior of the pristine bPEI-AuNPs in both the raw and filtered river water was consistent
41 with that observed previously.¹⁷ In the filtered river, the TR-DLS measurements water indicate a
42 near-instantaneous increase in D_h ($D_{h,30}/D_{h,0} = 1.82 \pm 0.18$ [\pm standard deviation; $n = 2$]), after
43 which no further changes in D_h were observed (Figure 2a and Supplementary Information Figure
44 S2c), while the PALS measurements indicate that the pristine bPEI-AuNPs underwent charge
45 reversal (Figure 2b). Taken together, these results are indicative of the rapid adsorption of NOM
46 to the cationic bPEI surface coating, resulting in the formation of an eco-corona.^{17, 36} This is
47 supported by the UV-Vis measurements in the filtered river water (Supplementary Figure S4c),
48 which show a red-shift in λ_{SPR} relative to that measured in DDI water and an increase in the FWHM
49
50
51
52
53
54
55

(Supplementary Information Tables S8 – S9). At the NOM-to-AuNP mass concentration ratio ([NOM]:[ENM]) and the NOM mass concentration-to-AuNP surface area ratio ([NOM]: ENM_{SA}) of the batch experiments (≈ 6.5 mg C/mg Au, ≈ 318 mg C/m², respectively) and the TR-DLS measurements (≈ 1.7 mg C/mg Au, ≈ 83 mg C/m², respectively), this eco-corona is expected to sufficiently cover the bPEI-AuNPs and prevent extensive homo- and heteroaggregation.^{17, 36} Indeed, the SEM micrographs do indicate that some homo- and heteroaggregation occurred, as evidenced by the relatively small aggregates that are observed, while monodispersed and isolated bPEI-AuNPs are still evident (Figure 2e). In combination, these results are in line with previous findings that as NOM adsorbs to the bPEI-AuNPs, NOM-facilitated interparticle bridging can cause the bPEI-AuNPs to aggregate. However, once the fractional surface coverage of adsorbed NOM becomes sufficiently high, further aggregation is prevented due to the electrosteric stability imparted by the eco-corona formed on the particles.^{17, 36}

In summary, the loss of the PEG-AuNPs in the raw river water is attributed to the elevated TSS concentration, the behavior of the COOH-AuNPs is unclear but consistent with that observed previously, and the colloidal stability of the bPEI-AuNPs is linked to eco-corona formation and the surface coverage of NOM on the AuNP surfaces (i.e., the [NOM]: ENM_{SA} ratio). The results using the filtered river water highlight the impact of eco-corona formation on ENM aggregation behavior and demonstrate the importance of the [NOM]: ENM_{SA} ratio. Likewise, the results using the raw river water highlight the impact that the number concentration ratio of background NCs-to-AuNPs ($N_{NC}:N_{ENM}$) has on aggregation behavior. More importantly for the current study, however, is that these results serve as a foundation for examining the aggregation behavior of the aged AuNPs in the same aquatic media.

Aged AuNPs in River Water

In general, changes in the physiochemical properties of each AuNP type during the aging process were consistent with those observed previously, indicating that each AuNP type was transformed in the filtered wastewater media.³⁷ Briefly, the D_h of all three AuNP types increased relative to their pristine analogs during the aging process, indicating that all three AuNP types homoaggregated in the filtered wastewater media (Figure 2a and Supplementary Information

1
2
3
4
5 Figure S3). Based on previous trends observed in the μ_E , UV-Vis spectra, and an analysis of TEM
6 micrographs, this behavior was attributed to the formation of an organic matter corona
7 comprised of extracellular polymeric substances (EPS) present in the wastewater treatment
8 system and the aquatic chemistry of that environment.³⁷ In the current work, the μ_E of the aged
9 AuNPs measured in the TFF permeate and filtered river water were comparable, consistently
10 negative, and indicate that the bPEI-AuNPs underwent charge reversal (Figure 2b). The UV-Vis
11 spectra of the aged AuNPs in the TFF permeate and filtered river water show that λ_{SPR} of each
12 aged AuNP type was red-shifted relative to that measured in DDI water (Supplementary
13 Information Table S8) and the FWHM increased (Supplementary Information Figure S4 and Table
14 S9). The aged COOH-AuNPs show a substantial increase in the FWHM and an accompanying
15 broadening of the peak at λ_{SPR} , likely due to the presence of a 'secondary' peak from the
16 transverse surface plasmon resonance (TSPR) overlapping with the 'primary' peak from the
17 longitudinal surface plasmon resonance (LSPR).^{39, 40} The presence of the LSPR and TSPR was
18 observed previously with the COOH-AuNPs.³⁷
19
20
21
22
23
24
25
26
27
28
29

30 After aging in the wastewater media, significant losses of all three AuNP types were observed in
31 the raw river water (PEG: paired t -test [$\eta = 6$], $p = 0.02$; COOH: paired t -test [$\eta = 6$], $p = 0.01$; bPEI:
32 paired t -test [$\eta = 6$], $p < 0.01$; Figure 1a, 1e, and 1i, respectively) and in the filtered river water
33 (PEG: paired t -test [$\eta = 6$], $p < 0.01$; COOH: paired t -test [$\eta = 4$], $p = 0.049$; bPEI: paired t -test [$\eta =$
34 6], $p = 0.04$; Figure 1c, 1g, and 1k, respectively). Limited AuNP removal was observed in the DDI
35 water controls (Figure 1d, 1h, and 1l, respectively), revealing that attachment to vessel walls and
36 loss via centrifugation were not responsible for the results observed in the river water.
37
38
39
40
41
42
43

44 The removal of the aged AuNPs is attributed to aggregation that occurred after their introduction
45 and continuous mixing in the river water. This is supported by the trends in η observed between
46 the raw, centrifuged, and filtered river water. In the raw river water, the loss of the aged AuNPs
47 were consistently higher than those measured in filtered river water and were either comparable
48 to or slightly greater than those observed in the centrifuged river water (Figure 1). Given that
49 aggregation rates are dependent on the particle number concentration, η would be expected to
50 be highest in the raw river water and lowest in the filtered river water, with the centrifuged river
51
52
53
54
55
56
57
58
59
60

1
2
3
4
5 water in between, due to differences in the number concentration of background particles in
6 these media. Likewise, greater removal in the raw and centrifuged river water, relative to the
7 filtered river water, indicates that the aged AuNPs underwent heteroaggregation, in addition to
8 homoaggregation, in these media due to the higher concentration of background particles.
9

10
11
12
13 This is further supported by comparing the DLS results of the aged AuNPs (Figure 2a and
14 Supplementary Information Figure S3) with the SEM micrographs obtained from the batch
15 experiments (Figure 2c-e). For the aged PEG-AuNPs, the DLS results show that the PEG-AuNPs
16 homoaggregated during aging to $D_{h,aged} \approx 130$ nm, which is indicative of particle aggregates mainly
17 comprised of doublets and triplets (Figure 2a and Supplementary Information Figure S3). This is
18 confirmed in the SEM micrographs collected from the raw, centrifuged, and filtered river water
19 (Figure 2c). While individual aged PEG-AuNPs are clearly evident in the filtered river water, many
20 appear in close proximity and are consistent with doublet and triplet particle aggregates
21 (highlighted in Figure 2c). In the raw and centrifuged river water, the aged PEG-AuNPs are mainly
22 associated with the background NCs. As a whole, these results confirm that the aged PEG-AuNPs
23 mainly heteroaggregated in the raw and centrifuged river water, undergoing minimal additional
24 homoaggregation beyond that which occurred while aging in the wastewater media. Likewise,
25 similar trends are observed between the DLS and SEM results for both the aged COOH- and bPEI-
26 AuNPs. Both these particle types homoaggregated during aging to $D_{h,aged} \approx 200 - 250$ nm (Figure
27 2a and Supplementary Information Figure S3) and the SEM micrographs confirm the presence of
28 large aggregate assemblages on the order of several hundred nanometers in the raw, centrifuged,
29 and filtered river water (highlighted in Figures 2d and 2e). In the raw and centrifuged river water,
30 many of these aggregate assemblages appear attached with or in close proximity to the
31 background NCs, indicative of heteroaggregation with the background NCs.
32
33
34
35
36
37
38
39
40
41
42
43
44
45

46
47 To elucidate the mechanisms that might explain the behavior of the aged AuNPs, a suite of long-
48 duration TR-DLS measurements were performed using the filtered river water, dialyzed river
49 water, and synthetic river water containing only ionic species. The dialyzed river water was used
50 to investigate homoaggregation via NOM-facilitated interparticle bridging, where the NOM in the
51 river water adsorbs directly to the corona and/or to divalent cations bound to the corona on an
52
53
54
55

1
2
3
4
5 aged AuNP and then subsequently attaches to other aged AuNPs via the same process. The
6 synthetic river water was used to examine homoaggregation via divalent cation bridging (DCB),
7 where the ionic charge of a divalent cation forms an electrostatic attachment between two aged
8 AuNPs. Homoaggregation via DCB could potentially be enhanced by the presence of divalent
9 cations already bound to the aged AuNP corona that were acquired in the filtered wastewater,
10 where divalent cation concentrations were much higher than those measured in the filtered river
11 water (Supplementary Information Tables S2 and S4). Lastly, the filtered river water was used as
12 a reference since both NOM and divalent cations are present in the media and both mechanisms
13 could potentially occur.
14
15
16
17
18
19
20
21

22 The extent of aggregation ($D_{h,60}/D_{h,0}$) of each aged AuNP type in both the dialyzed and synthetic
23 river water did not differ substantially from that measured in the filtered river water (Figure 3).
24 This was consistent across all three aged AuNP types and indicates that the aged AuNPs did not
25 undergo continued homoaggregation in the river water (i.e., homoaggregation beyond that which
26 occurred while aging in the wastewater media [Figure 2a]). Thus, neither NOM-facilitated
27 interparticle bridging nor DCB could be attributed as the dominant mechanism driving the
28 behavior of the aged AuNPs in the river water.
29
30
31
32
33
34
35
36
37
38
39
40
41
42
43
44
45
46
47
48
49
50
51
52
53
54
55
56
57
58
59
60

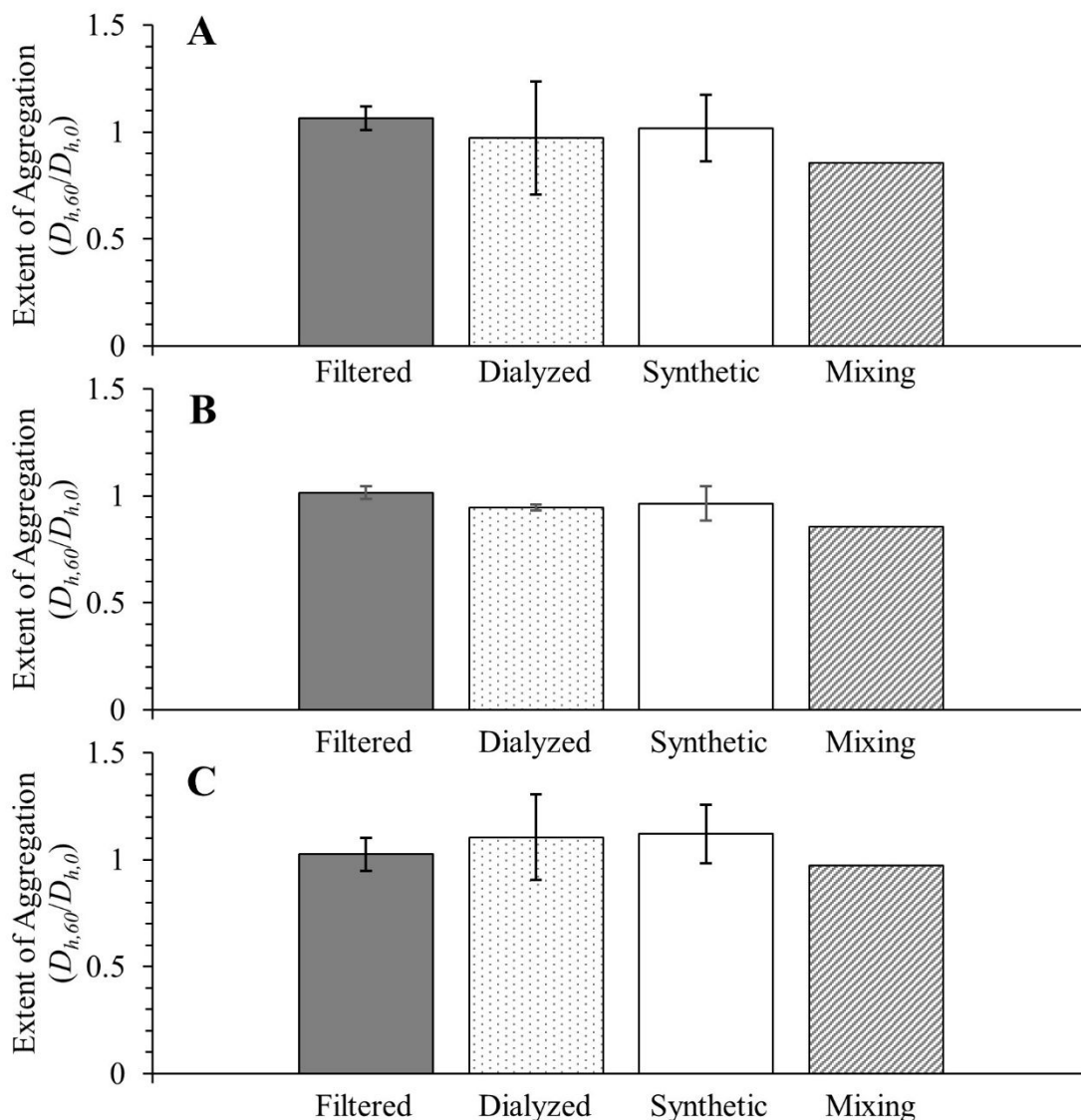


Figure 3. Extent of aggregation ($D_{h,60}/D_{h,0}$) of aged (a) PEG-AuNPs, (b) COOH-AuNPs, and (c) bPEI-AuNPs in filtered river water, dialyzed river water, synthetic river water containing only ionic species, and after mixing per the batch experiment method. Error bars indicate \pm 95% confidence interval ($n = 3$; filtered, dialyzed, and ionic only).

A final mechanism that was also explored was the impact of additional particle-particle collisions that the aged AuNPs undergo during the batch experiments due to fluid shear via the continuous mixing. Given that the D_h of the aged AuNPs when they were first dispersed in the filtered river water was on the order of 100 – 250 nm (Supplementary Information Figure S3), the initial particle-particle interactions between the aged AuNPs would predominantly be from Brownian

1
2
3
4
5 motion.^{41, 42} However, as the aged AuNPs homoaggregate and their D_h increases, shear-induced
6 collisions could become more prevalent.^{41, 42} However, the D_h of each aged AuNP type was not
7 found to substantially increase, relative to the D_h after aging, after continuously mixing in the
8 filtered river water at the same speed and duration as that used during the batch experiments
9 (Figure 3). Thus, the mixing during the batch experiments does not appear to drive the behavior
10 of the aged AuNPs in the river water.
11
12
13
14
15

16
17 Overall, in comparing the results observed with the aged AuNPs relative to their pristine
18 counterparts, the impact that the transformations during wastewater treatment have on the
19 aggregation behavior of the model ENMs in real aquatic media is apparent. In their pristine form,
20 only the COOH-AuNPs in filtered river water and the PEG-AuNPs in raw river water were found to
21 undergo significant aggregation and subsequent sedimentation. In contrast, after aging in the
22 wastewater media, significant loss of each aged AuNP type was observed in both the filtered and
23 raw river water, with higher losses observed in the latter. This finding demonstrates that the
24 physiochemical properties of aged ENMs, which are dictated by the organic matter corona
25 acquired by the ENMs during exposure to the wastewater media, will control their aggregation
26 behavior in the environment rather than the physiochemical properties the ENMs initially possess
27 in their pristine form. In particular, we find that for the three AuNP types investigated in the
28 current work, the physiochemical properties of the aged ENMs enabled their heteroaggregation
29 in river water, while no further homoaggregation beyond that which occurred during the aging
30 process was observed.
31
32
33
34
35
36
37
38
39
40
41

42 Furthermore, the previous and current work indicate that the initial properties of the ENM surface
43 coatings can alter the transformations occurring during wastewater treatment. Functionally, the
44 impact of these transformations is consistent across the AuNP types investigated (i.e., increased
45 loss from suspension). However, it is unclear whether the composition of the organic matter
46 corona acquired by the different AuNP types is similar or varies due to differences in the initial
47 physiochemical properties of the engineered surface coatings. As noted previously, additional
48 work is needed to reveal the nature of the corona formed on the AuNPs during exposure to the
49 wastewater media.³⁷
50
51
52
53
54

Implications for Examining ENM Environmental Fate

Based on previous research and the results presented in the current work, several conclusions can be reached. First, ENM transformations that occur prior to their release and the properties that result will dictate ENM behavior in the environment. With regards to the engineered surface coatings examined here, their influence on ENM fate in natural aquatic media is negligible after aging in wastewater. Instead, the organic matter corona acquired by the ENMs in wastewater treatment systems will dictate ENM interactions in natural aquatic environments. It remains to be determined whether the aged ENMs will undergo additional transformations once released to the environment, such as replacement or overcoating of the wastewater-derived corona layer by NOM in the receiving water.

Second, while the release of pristine ENMs to the environment is unlikely, these particles are nonetheless an important tool for helping elucidate the processes impacting the environmental fate of ENMs. For example, this study provides additional evidence that the aggregation behavior of ENMs in the environment is linked to the relative concentrations of NOM, background NCs and ENMs (i.e., $[NOM]:N_{NC}:N_{ENM}$), an important insight that was identified by examining the aggregation behavior of pristine ENMs in both synthetic and real aquatic media. However, in light of the first conclusion, it is important to recognize the inherent limitations of using pristine ENMs. Given that these particle types are not representative of those released to the environment, researchers should be cautious when applying the findings derived using pristine ENMs in simplified aquatic media to predict ENM behavior under more realistic conditions.

With the intent of refining ENM environmental fate models, it is recommended that future research focus on further elucidating the behavior of aged ENMs in real aquatic media. Ultimately, this line of inquiry should work towards establishing the factors that dictate the outcome of medium-dependent processes, such as aggregation, and how those factors are incorporated in ENM environmental fate models. To achieve this, it is envisioned that both pristine and aged ENMs will be used, ideally with ENMs aged through a variety of lab-based procedures that mimic

1
2
3
4
5 a variety of relevant transformation processes that ENMs might undergo during their various life
6 stages (i.e., production, use, and disposal).
7
8
9

10 **CONFLICTS OF INTEREST**

11
12
13 There are no conflicts of interest to declare.
14
15
16

17 **ACKNOWLEDGEMENTS**

18
19 This research was supported by the National Science Foundation (NSF) Graduate Research
20 Fellowship Program under Grant No. DGE-1314109 and NSF Grant No. 1255020. Any opinions,
21 findings, and conclusions or recommendations expressed in this material are those of the
22 author(s) and do not necessarily reflect the views of the NSF. Special thanks to A. Franco (Portland
23 State University Trace Element Analysis Laboratory) for assistance with the ICP-MS
24 measurements; K. Motter (Institute for Water and Watersheds Collaboratory) for assistance with
25 TOC/DOC measurements; and I. Ramirez-Aguilar for assistance with the DLS, PALS, and UV-Vis
26 measurements.
27
28
29
30
31
32
33
34
35
36
37
38
39
40
41
42
43
44
45
46
47
48
49
50
51
52
53
54
55
56
57
58
59
60

REFERENCES

1. A. A. Keller, S. McFerran, A. Lazareva and S. Suh, Global life cycle releases of engineered nanomaterials, *J. Nanopart. Res.*, 2013, **15**.
2. A. A. Keller, W. Vosti, H. Wang and A. Lazareva, Release of engineered nanomaterials from personal care products throughout their life cycle, *J. Nanopart. Res.*, 2014, **16**.
3. S. J. Klaine, P. J. Alvarez, G. E. Batley, T. F. Fernandes, R. D. Handy, D. Y. Lyon, S. Mahendra, M. J. McLaughlin and J. R. Lead, Nanomaterials in the environment: behavior, fate, bioavailability, and effects, *Environ. Toxicol. Chem.*, 2008, **27**, 1825-1851.
4. N. Mahaye, M. Thwala, D. A. Cowan and N. Musee, Genotoxicity of metal based engineered nanoparticles in aquatic organisms: A review, *Mutat Res*, 2017, **773**, 134-160.
5. H. H. Liu and Y. Cohen, Multimedia environmental distribution of engineered nanomaterials, *Environ. Sci. Technol.*, 2014, **48**, 3281-3292.
6. J. A. Meesters, A. A. Koelmans, J. T. Quik, A. J. Hendriks and D. van de Meent, Multimedia modeling of engineered nanoparticles with SimpleBox4nano: model definition and evaluation, *Environ. Sci. Technol.*, 2014, **48**, 5726-5736.
7. K. L. Garner, S. Suh and A. A. Keller, Assessing the Risk of Engineered Nanomaterials in the Environment: Development and Application of the nanoFate Model, *Environ. Sci. Technol.*, 2017, **51**, 5541-5551.
8. W. J. G. M. Peijnenburg, M. Baalousha, J. Chen, Q. Chaudry, F. Von der kammer, T. A. J. Kuhlbusch, J. Lead, C. Nickel, J. T. K. Quik, M. Renker, Z. Wang and A. A. Koelmans, A Review of the Properties and Processes Determining the Fate of Engineered Nanomaterials in the Aquatic Environment, *Crit. Rev. Env. Sci. Technol.*, 2015, **45**, 2084-2134.
9. M. Baalousha, Effect of nanomaterial and media physicochemical properties on nanomaterial aggregation kinetics, *NanoImpact*, 2017, **6**, 55-68.
10. E. M. Hotze, T. Phenrat and G. V. Lowry, Nanoparticle aggregation: challenges to understanding transport and reactivity in the environment, *J. Environ. Qual.*, 2010, **39**, 1909-1924.
11. S. M. Louie, R. D. Tilton and G. V. Lowry, Critical review: impacts of macromolecular coatings on critical physicochemical processes controlling environmental fate of nanomaterials, *Environ. Sci.: Nano*, 2016, **3**, 283-310.
12. S. M. Louie, R. D. Tilton and G. V. Lowry, Effects of molecular weight distribution and chemical properties of natural organic matter on gold nanoparticle aggregation, *Environ. Sci. Technol.*, 2013, **47**, 4245-4254.
13. S. Jayalath, S. C. Larsen and V. H. Grassian, Surface adsorption of Nordic aquatic fulvic acid on amine-functionalized and non-functionalized mesoporous silica nanoparticles, *Environ. Sci.: Nano*, 2018, **5**, 2162-2171.
14. B. P. Espinasse, N. K. Geitner, A. Schierz, M. Therezien, C. J. Richardson, G. V. Lowry, L. Ferguson and M. R. Wiesner, Comparative Persistence of Engineered Nanoparticles in a Complex Aquatic Ecosystem, *Environ. Sci. Technol.*, 2018, **52**, 4072-4078.
15. D. L. Slomberg, P. Ollivier, H. Miche, B. Angeletti, A. Bruchet, M. Philibert, J. Brant and J. Labille, Nanoparticle stability in lake water shaped by natural organic matter properties and presence of particulate matter, *Sci. Total Environ.*, 2019, **656**, 338-346.
16. N. K. Geitner, N. J. O'Brien, A. A. Turner, E. J. Cummins and M. R. Wiesner, Measuring Nanoparticle Attachment Efficiency in Complex Systems, *Environ. Sci. Technol.*, 2017, **51**, 13288-13294.
17. M. C. Surette and J. A. Nason, Nanoparticle aggregation in a freshwater river: the role of engineered surface coatings, *Environ. Sci.: Nano*, 2019, **6**, 540-553.
18. J. T. Quik, I. Velzeboer, M. Wouterse, A. A. Koelmans and D. van de Meent, Heteroaggregation and sedimentation rates for nanomaterials in natural waters, *Water Res.*, 2014, **48**, 269-279.

- 1
 - 2
 - 3
 - 4
 - 5
 - 6
 - 7
 - 8
 - 9
 - 10
 - 11
 - 12
 - 13
 - 14
 - 15
 - 16
 - 17
 - 18
 - 19
 - 20
 - 21
 - 22
 - 23
 - 24
 - 25
 - 26
 - 27
 - 28
 - 29
 - 30
 - 31
 - 32
 - 33
 - 34
 - 35
 - 36
 - 37
 - 38
 - 39
 - 40
 - 41
 - 42
 - 43
 - 44
 - 45
 - 46
 - 47
 - 48
 - 49
 - 50
 - 51
 - 52
 - 53
 - 54
 - 55
 - 56
 - 57
 - 58
 - 59
 - 60
19. M. R. Esfahani, V. L. Pallem, H. A. Stretz and M. J. M. Wells, Core-size regulated aggregation/disaggregation of citrate-coated gold nanoparticles (5-50nm) and dissolved organic matter: Extinction, emission, and scattering evidence, *Spectrochim Acta A Mol Biomol Spectrosc*, 2018, **189**, 415-426.
20. H. E. Hadri, S. M. Louie and V. A. Hackley, Assessing the interactions of metal nanoparticles in soil and sediment matrices - A quantitative analytical multi-technique approach, *Environ Sci Nano*, 2018, **5**.
21. J. Liu, S. Legros, F. von der Kammer and T. Hofmann, Natural organic matter concentration and hydrochemistry influence aggregation kinetics of functionalized engineered nanoparticles, *Environ. Sci. Technol.*, 2013, **47**, 4113-4120.
22. G. V. Lowry, K. B. Gregory, S. C. Apte and J. R. Lead, Transformations of nanomaterials in the environment, *Environ. Sci. Technol.*, 2012, **46**, 6893-6899.
23. U. Weilenmann, C. R. Omelia and W. Stumm, Particle-Transport in Lakes - Models and Measurements, *Limnol. Oceanogr.*, 1989, **34**, 1-18.
24. J. Buffle and G. G. Leppard, Characterization of aquatic colloids and macromolecules. 1. Structure and behavior of colloidal material, *Environ. Sci. Technol.*, 1995, **29**, 2169-2175.
25. J. Buffle, K. J. Wilkinson, S. Stoll, M. Filella and J. W. Zhang, A generalized description of aquatic colloidal interactions: The three-colloidal component approach, *Environ. Sci. Technol.*, 1998, **32**, 2887-2899.
26. L. K. Limbach, R. Bereiter, E. Muller, R. Krebs, R. Galli and W. J. Stark, Removal of oxide nanoparticles in a model wastewater treatment plant: influence of agglomeration and surfactants on clearing efficiency, *Environ. Sci. Technol.*, 2008, **42**, 5828-5833.
27. H. P. Jarvie, H. Al-Obaidi, S. M. King, M. J. Bowes, M. J. Lawrence, A. F. Drake, M. A. Green and P. J. Dobson, Fate of silica nanoparticles in simulated primary wastewater treatment, *Environ. Sci. Technol.*, 2009, **43**, 8622-8628.
28. R. Kaegi, A. Voegelin, C. Ort, B. Sinnet, B. Thalmann, J. Krismer, H. Hagendorfer, M. Elumelu and E. Mueller, Fate and transformation of silver nanoparticles in urban wastewater systems, *Water Res.*, 2013, **47**, 3866-3877.
29. L. Otero-Gonzalez, J. A. Field, I. A. C. Calderon, C. A. Aspinwall, F. Shadman, C. Zeng and R. Sierra-Alvarez, Fate of fluorescent core-shell silica nanoparticles during simulated secondary wastewater treatment, *Water Res.*, 2015, **77**, 170-178.
30. R. Kaegi, A. Voegelin, B. Sinnet, S. Zuleeg, H. Hagendorfer, M. Burkhardt and H. Siegrist, Behavior of metallic silver nanoparticles in a pilot wastewater treatment plant, *Environ. Sci. Technol.*, 2011, **45**, 3902-3908.
31. B. Kim, C. S. Park, M. Murayama and M. F. Hochella, Discovery and characterization of silver sulfide nanoparticles in final sewage sludge products, *Environ. Sci. Technol.*, 2010, **44**, 7509-7514.
32. L. Li, M. Stoiber, A. Wimmer, Z. Xu, C. Lindenblatt, B. Helmreich and M. Schuster, To What Extent Can Full-Scale Wastewater Treatment Plant Effluent Influence the Occurrence of Silver-Based Nanoparticles in Surface Waters?, *Environ. Sci. Technol.*, 2016, **50**, 6327-6333.
33. M. A. Kiser, P. Westerhoff, T. Benn, Y. Wang, J. Perez-Rivera and K. Hristovski, Titanium nanomaterial removal and release from wastewater treatment plants, *Environ. Sci. Technol.*, 2009, **43**, 6757-6763.
34. P. Westerhoff, G. Song, K. Hristovski and M. A. Kiser, Occurrence and removal of titanium at full scale wastewater treatment plants: implications for TiO₂ nanomaterials, *J. Environ. Monit.*, 2011, **13**, 1195-1203.
35. F. Loosli, J. Wang, S. Rothenberg, M. Bizimis, C. Winkler, O. Borovinskaya, L. Flamigni and M. Baalousha, Sewage spills are a major source of titanium dioxide engineered (nano)-particle release into the environment, *Environ. Sci.: Nano*, 2019, **6**, 763-777.

- 1
- 2
- 3
- 4
- 5 36. M. C. Surette and J. A. Nason, Effects of surface coating character and interactions with natural
- 6 organic matter on the colloidal stability of gold nanoparticles, *Environ. Sci.: Nano*, 2016, **3**, 1144-
- 7 1152.
- 8 37. M. C. Surette, J. A. Nason and R. Kaegi, The influence of surface coating functionality on the aging
- 9 of nanoparticles in wastewater, *Environ Sci-Nano*, 2019, **6**, 2470-2483.
- 10 38. F. N. Ponnampuruma, E. M. Tianco and T. A. Loy, Ionic Strengths of the Solutions of Flooded Soils
- 11 and Other Natural Aqueous Solutions from Specific Conductance, *Soil Science*, 1966, **102**, 408-413.
- 12 39. W. Rechberger, A. Hohenau, A. Leitner, J. R. Krenn, B. Lamprecht and F. R. Aussenegg, Optical
- 13 properties of two interacting gold nanoparticles, *Optics Communications*, 2003, **220**, 137-141.
- 14 40. I. E. Sendroiu, S. F. Mertens and D. J. Schiffrin, Plasmon interactions between gold nanoparticles in
- 15 aqueous solution with controlled spatial separation, *Phys. Chem. Chem. Phys.*, 2006, **8**, 1430-1436.
- 16 41. M. Han and D. F. Lawler, Interactions of Two Settling Spheres: Settling Rates and Collision
- 17 Efficiency, *Journal of Hydraulic Engineering*, 1991, **117**, 1269-1289.
- 18 42. M. Y. Han and D. F. Lawler, The (Relative) Insignificance of G in Flocculation, *J Am Water Works*
- 19 *Ass*, 1992, **84**, 79-91.
- 20
- 21
- 22
- 23
- 24
- 25
- 26
- 27
- 28
- 29
- 30
- 31
- 32
- 33
- 34
- 35
- 36
- 37
- 38
- 39
- 40
- 41
- 42
- 43
- 44
- 45
- 46
- 47
- 48
- 49
- 50
- 51
- 52
- 53
- 54
- 55
- 56
- 57
- 58
- 59
- 60